

## Determination of the $P_{In}$ antisite structure in InP by optically detected electron-nuclear double resonance

D. Y. Jeon, H. P. Gislason,\* J. F. Donegan, and G. D. Watkins  
*Department of Physics, Sherman Fairchild Laboratory, Lehigh University,  
 Bethlehem, Pennsylvania 18015*

(Received 17 April 1987)

Optically detected electron-nuclear double resonance (ODENDOR) is reported for the  $P_{In}$  antisite in  $p$ -type InP. In both electron-irradiated and as-grown samples, ENDOR signals from the four nearest P neighbors and the next In shell were detected by monitoring radio-frequency-induced changes in magnetic circular dichroism associated with absorption near the band edge of InP while maintaining microwave resonance of the  $P_{In}$  antisite. The electronic wave function of the  $P_{In}^+$  state is highly localized, essentially all of it accounted for within these first two neighbor shells. The optical-absorption band associated with the antisite is centered above the InP band gap, and only its tail is observed.

An intrinsic defect believed to be important in III-V compound semiconductors is the anion antisite, where a group-V atom occupies a group-III atom site, forming a double donor.<sup>1</sup> The first experimental evidence of this defect was for the  $P_{Ga}$  antisite in GaP, where via EPR<sup>2</sup> and optically detected magnetic resonance<sup>3,4</sup> (ODMR), the isotropic central P hyperfine (hf) interaction plus the anisotropic hyperfine interaction of four equivalent phosphorus near neighbors were resolved.

Similar spectra have subsequently been reported for GaAs (Refs. 5 and 6) and InP;<sup>7-9</sup> however, only the central hyperfine interactions could be resolved. In these cases, therefore, confirmation of the antisite identification requires electron-nuclear double resonance<sup>10</sup> (ENDOR) to probe the near-neighbor environment. Such a study has been reported for the  $As_{Ga}$  antisite in GaAs, using optical detection of electron-nuclear double resonance via magnetic circular dichroism in absorption<sup>11</sup> (MCD-ODENDOR), where the four nearest-neighbor As environment has been confirmed.

In this Rapid Communication, we report MCD-ODENDOR results on the InP-related center. We confirm the presence of four nearest-neighbor phosphorus atoms. In addition, we detect hyperfine interactions with the second-nearest-neighbor In shell.

The two samples used in this investigation were liquid-encapsulated Czochralski (LEC)  $p$ -type InP crystals doped with Zn. The first sample had a thickness of 500  $\mu\text{m}$ , a hole concentration of  $3 \times 10^{17}/\text{cm}^3$ , and was irradiated at room temperature by a 2.5-MeV electron beam to a fluence of  $1.0 \times 10^{17} \text{ e}^-/\text{cm}^2$ . The sample was subsequently annealed at 100°C for 2 h to increase the intensity of the ODMR signal. The second sample had a thickness of 300  $\mu\text{m}$ , a hole concentration of  $1.2 \times 10^{16}/\text{cm}^3$ , and was studied in its as-grown state.

The MCD, ODMR, and ODENDOR experiments were performed at pumped-liquid-He temperatures in an Oxford Instruments SM-4 superconducting magnet optical cryostat. Samples were mounted in a 35-GHz TE<sub>011</sub> cavity having the form of concentric rings for easy optical ac-

cess.<sup>12</sup> The light source was a 600-W tungsten halogen lamp dispersed by a  $\frac{1}{4}$ -m Jarrel-Ash monochromator. Alternating right and left circularly polarized components of the light were generated by a linear polarizer (Polaroid HR) in conjunction with a quartz stress modulator (Hinds PEM-3) operating at 50.3 kHz. The transmitted light propagating along the static magnetic field direction was monitored by a fast Ge detector (North Coast EO-817P), the difference between the right and left components being obtained by lock-in detection at 50.3 kHz.

The MCD can be defined as  $\alpha_L - \alpha_R$ , the difference in absorption coefficients for left and right circularly polarized light propagating along the static magnetic field direction. In our samples,  $(\alpha_L - \alpha_R)d \ll 1$ , where  $d$  is the sample thickness, and to a very good approximation; therefore,

$$\alpha_L - \alpha_R = \frac{2(I_R - I_L)}{(I_R + I_L)d}, \quad (1)$$

where  $I_R$  and  $I_L$  are the transmitted right and left circularly polarized components, respectively. All values given for the MCD in this paper were determined in the above manner, the lock-in signal (proportional to  $I_R - I_L$ ) being divided by the average transmitted light. In this way, the spectral response of the light source, monochromator, detector, lenses, windows, etc., were automatically corrected for.

For the ODMR experiment one monitors changes in MCD induced by microwave transitions in the ground state. The ODMR spectrum was obtained by monitoring the MCD signal while sweeping the magnetic field at a fixed microwave frequency. For the ODENDOR experiment a two-turn coil was installed in the cavity such that its magnetic field axis was perpendicular to the static and microwave magnetic fields. The radio frequency was generated by a frequency synthesizer (Fluke 6060B) which was controlled by an IBM 9000 computer through an IEEE interface bus. The output of the synthesizer was then amplified by an rf power amplifier (ENI 3100 LA). The ODENDOR spectrum was obtained by monitoring

changes in the ODMR intensity versus radio frequency at microwave resonance, with signal averaging being performed as necessary by the computer.

Figure 1 shows the ODMR spectrum from both the as-grown and the electron-irradiated samples, obtained by monitoring the MCD in absorption just below the band edge. The microwave-induced change of the MCD shows the characteristic two-line spectrum expected for a phosphorus antisite as given by the  $S = \frac{1}{2}$ -spin Hamiltonian

$$\mathcal{H} = g\mu_B \mathbf{S} \cdot \mathbf{B} + a_0 \mathbf{I} \cdot \mathbf{S} + \sum_i \mathbf{I}_i \cdot \tilde{\mathbf{A}}_i \cdot \mathbf{S} \quad (2)$$

where the second term describes the hyperfine interaction with the central P atom, and the third term the interaction with nuclei on neighboring atomic sites. For both samples, the measured central P hf splitting  $a_0 = (980 \pm 20) \times 10^{-4} \text{ cm}^{-1}$  and  $g = 2.000 \pm 0.003$  agree, within experimental error, with those previously measured by EPR<sup>7</sup> and ODMR.<sup>8,9</sup> Hyperfine interactions with nuclei on neighboring atomic sites are not resolved, contributing presumably only to the width of the lines.

To deduce the shape of the MCD band responsible for this ODMR, the spectral dependence was measured by scanning the wavelength of the incident light while observing the maximum ODMR signal (see Fig. 2). To eliminate the MCD background, the microwaves were also on-off modulated at 1 Hz in this case, with a second lock-in detector. We conclude from Fig. 2 that for both samples the peak of the MCD absorption band is above the band gap, only the low-energy tail of the band being seen. This differs from previously reported results, which identified the MCD band as centered at  $0.93 \mu\text{m}$ .<sup>8</sup> In

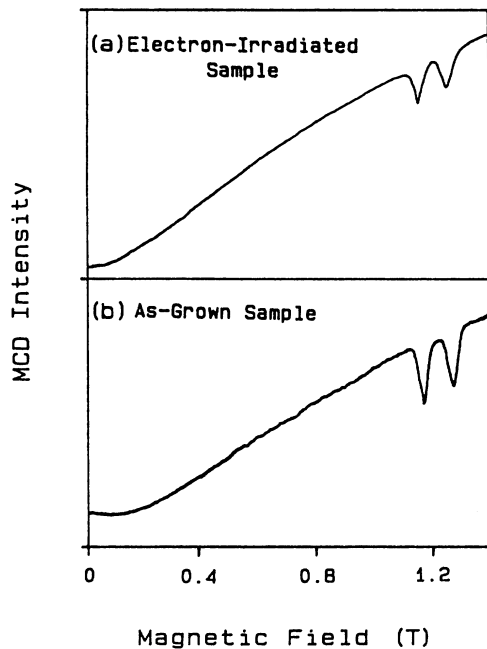


FIG. 1. The ODMR spectrum of the P<sub>1n</sub> antisite in InP with  $\mathbf{B} \parallel [100]$  at  $T = 1.7 \text{ K}$  and  $\nu = 35.0 \text{ GHz}$ . The gain for (b) has been increased by a factor of 4.

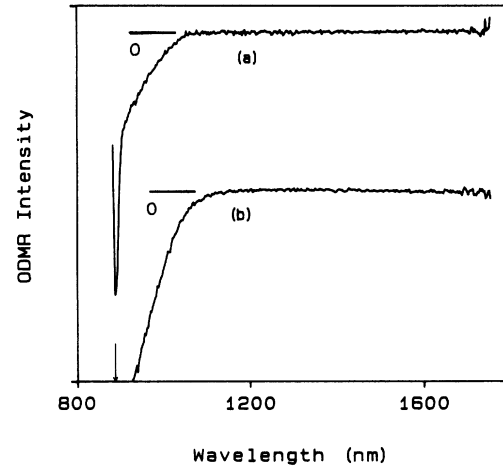


FIG. 2. The spectral dependence (corrected for detector and monochromator responses) of the P<sub>1n</sub> antisite ODMR spectrum: (a) as-grown sample, (b) electron-irradiated sample. The band gap of InP is indicated by an arrow.

these previous studies, correction for the system response was not included. We find that it is essential to divide by  $I_R + I_L$ , Eq. (1), the maximum ODMR signal near  $0.93 \mu\text{m}$  being an artifact of the strongly decreased transmission near the band edge. This is particularly true for the electron-irradiated sample which has greatly increased absorption near the band edge and gives a maximum ODMR signal at  $\sim 0.98 \mu\text{m}$ .

In order to resolve the near-neighbor hyperfine structure, the change in ODMR was monitored by scanning the radio frequency from 0 to 200 MHz. Figure 3 shows

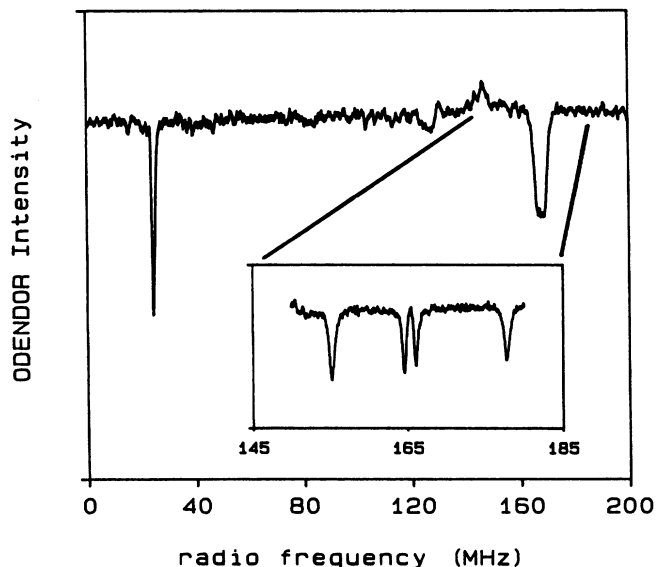


FIG. 3. The ODENDOR spectrum of the P<sub>1n</sub> antisite with  $\mathbf{B} \parallel [100]$  at  $B = 1.19 \text{ T}$  and  $T = 1.7 \text{ K}$ . The inset shows the P lines with  $\mathbf{B} \parallel [100] + 10^\circ$ .

the resulting ENDOR spectrum when  $B$  is set to the low-field transition and oriented along the  $[100]$  axis of the sample. For both samples, two sets of ENDOR transitions were detected, one at  $\sim 23$  MHz, the other at  $\sim 165$  MHz. The spectra were analyzed with the nuclear spin Hamiltonian

$$\mathcal{H}_n = \sum_i I_i \cdot \left( \tilde{A}_i \cdot \frac{M}{B} - \frac{\mu_i}{I_i} \right) \mathbf{B} + \sum_i I_i \cdot \tilde{Q} \cdot I_i + \sum_{i,j} I_i \cdot \tilde{D}_{ij} \cdot I_j, \quad (3)$$

for the electronic state with azimuthal quantum number  $M$ . Equation (3) results directly from Eq. (2), expanded to include a nuclear quadrupole interaction when  $I_i > \frac{1}{2}$  and the direct interaction of the  $i$ th nucleus with the external field  $\mathbf{B}$ . The first term contains the first-order magnetic interaction of each nucleus with its hyperfine and external fields. The last term arises from terms second order in  $A_i/g\mu_B B$  with

$$\tilde{D}_{ij} = \tilde{A}_i \cdot \sum_{M'} \frac{\langle M | \mathbf{S} | M' \rangle \langle M' | \mathbf{S} | M \rangle}{E_M - E_{M'}} \cdot \tilde{A}_j. \quad (4)$$

Written in this form, this includes not only the usual second-order corrections for a single nucleus ( $i=j$ ) but also the pseudo-dipole-dipole interaction<sup>13</sup> between different nuclei surrounding a common center.

From the dependence of each transition on  $B$ , the nuclear gyromagnetic ratio ( $\mu_i/I_i\hbar$ ) was measured and the nuclear species identified. The low-frequency set arises from  $^{113,115}\text{In}$  ( $+9.3 \pm 0.5$  MHz/T), the high-frequency set from  $^{31}\text{P}$  ( $+18 \pm 1$  MHz/T).

The angular dependence of the P lines is shown in Fig. 4. It reveals the characteristic four-line spectrum of four equivalent P atoms each with a different  $\langle 111 \rangle$  axis of

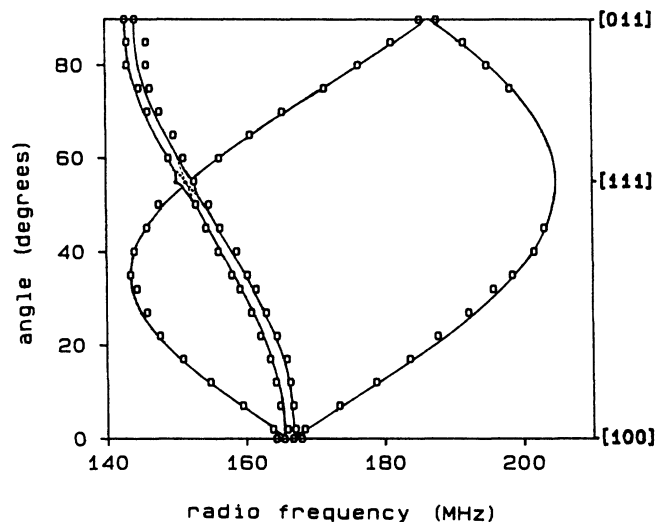


FIG. 4. The angular dependence of the ODENDOR lines,  $\mathbf{B} \perp [0\bar{1}1]$ . The points are the experimental data and the lines are a theoretical fit based on the spin Hamiltonian in Eq. (3).

symmetry. Analysis gives  $|A_{\parallel}| = 367.3 \pm 0.2$  MHz and  $|A_{\perp}| = 244.3 \pm 0.2$  MHz, with both of the same sign.

The pseudo-dipole-dipole terms given by Eq. (4) provide off-diagonal coupling between the product  $|m_i\rangle$  nuclear spin states which produce additional spectral splittings whenever the first-order terms of two nuclei are equal. These are included in the theoretical curves of Fig. 4 and the match with experiment is very good. The observation of these splittings confirms that all four P hyperfine interactions do indeed occur at a common center. From these results, we can conclude that the central phosphorus atom is surrounded by a tetrahedron of four equivalent phosphorus neighbors.

The In ENDOR resonance set at  $\sim 23$  MHz is almost isotropic giving  $\tilde{A} \sim a\bar{1}$ , with  $|a| = 23 \pm 2$  MHz. A small, partially resolved anisotropy is evident, however, and is currently under study. Although the analysis is not complete, the general pattern of the angular dependence appears roughly consistent with  $C_{1h}$  symmetry, as expected for each of the 12 atoms in the nearest In shell surrounding the substitutional  $\text{P}_{\text{In}}$  antisite.

The central  $\text{P}_{\text{In}}$  hf interaction is  $\sim 26\%$  of that predicted for a  $3s$  unpaired electron on a neutral phosphorus atom.<sup>14</sup> A similar estimate from our ENDOR results gives  $\sim 2.6\%$   $3s$  and  $\sim 13.1\%$   $3p$  on each of the four P neighbors and  $\sim 0.2\%$   $5s$  and  $\sim 0.6\%$   $5p$  on each of the twelve In next neighbors.<sup>15</sup> Viewed, therefore, as a linear combination of atomic orbitals (LCAO) centered on the atoms near the defect, the unpaired electron is  $\sim 26\%$  on the central  $\text{P}_{\text{In}}$ ,  $\sim 63\%$  on the first P shell, and  $\sim 10\%$  on the next In shell. The wave function is therefore highly localized ("deep") with essentially all of it accounted for within the first two neighbor shells. The distribution is very similar to that deduced for the  $\text{P}_{\text{Ga}}$  defect in GaP ( $\sim 26\%$  on  $\text{P}_{\text{Ga}}$ ,  $\sim 66\%$  on the four nearest phosphorus neighbors).<sup>16</sup>

The linewidths of the phosphorus ENDOR lines are  $\sim 0.5$  MHz. Although this is only  $\sim 0.2\%$  of the hyperfine coupling, it is still an order of magnitude greater than can be accounted for from direct or indirect [Eq. (4)] dipole-dipole interactions with neighboring nuclei. This indicates that the antisites may be perturbed slightly either by long-range strain and/or electric fields in the crystal, or by nearby charge compensating defects. Evidence of the first is the observation of broader ENDOR lines in the electron-irradiated sample. Evidence of the second can be inferred from the In ENDOR, where a very weak additional resolved structure has been detected near the strong In resonance at  $\sim 23$  MHz [the In nucleus has  $I = \frac{9}{2}$  and a sizable quadrupole moment, making it particularly sensitive to the presence of a nearby defect through the quadrupole term in Eq. (3)].

In any event, the perturbation is clearly small and we conclude that as far as the electronic structure of the defect is concerned, we are, for all practical purposes, measuring the properties of an isolated  $\text{P}_{\text{In}}$  antisite.<sup>17</sup>

Finally, we mention two interesting observations: (i) Although the MCD signal was a factor of 4 greater in the electron-irradiated material, the ODMR signal was only 50% greater and the ENDOR signals were essentially the same as for the as-grown material. This suggests that

more than one antisite-related defect may be present and that electron-irradiation may not introduce the same relatively unperturbed  $P_{In}$  antisite that is being observed by ODENDOR. (ii) Equation (3) predicts two ENDOR transitions for each nucleus, one from each of the two  $M = \pm \frac{1}{2}$ -spin states. The expected position for the other In resonance is close to 0 MHz and might be difficult to detect. The predicted positions for the corresponding P resonances, however, are  $\sim 126$  MHz, well within our measurement range. The failure to detect these suggests nuclear polarization effects<sup>18</sup> in the presence of the simultaneous EPR and ENDOR transitions. Additional evidence of this is the large ODENDOR effects ( $\sim 30$ – $45\%$

change in the ODMR signal). In conventional ENDOR, the signal is often only a few percent of the EPR signal.

In conclusion, we have resolved by ODENDOR the hyperfine interactions of the nearest-phosphorus and second-nearest In shell surrounding the  $P_{In}$  antisite in InP. This confirms its identification. The corresponding optical absorption MCD band is centered above the band gap of InP and only its low-energy tail is being observed.

We thank Dr. K. Ando for supplying the InP samples used in this study. This research was supported by the National Science Foundation under Grant No. DMR-85-20269.

\*Present address: Science Institute, University of Iceland, Dunhaga 3, 107 Reykjavik, Iceland.

<sup>1</sup>J. A. Van Vechten, *J. Electrochem. Soc.* **122**, 423 (1975).

<sup>2</sup>U. Kaufmann, J. Schneider, and A. Rauber, *Appl. Phys. Lett.* **29**, 312 (1976).

<sup>3</sup>K. P. O'Donnell, K. M. Lee, and G. D. Watkins, *Solid State Commun.* **44**, 1015 (1982).

<sup>4</sup>N. Killoran, B. C. Cavenett, M. Godlewski, T. A. Kennedy, and N. D. Wilsey, *J. Phys. C* **15**, L723 (1982).

<sup>5</sup>R. J. Wagner, J. J. Krebs, G. H. Stauss, and A. M. White, *Solid State Commun.* **36**, 15 (1980).

<sup>6</sup>B. K. Meyer, J.-M. Spaeth, and M. Scheffler, *Phys. Rev. Lett.* **52**, 851 (1984).

<sup>7</sup>T. A. Kennedy and N. D. Wilsey, *Appl. Phys. Lett.* **44**, 1089 (1984).

<sup>8</sup>M. Deiri, A. Kana-ah, B. C. Cavenett, T. A. Kennedy, and N. D. Wilsey, *J. Phys. C* **17**, L793 (1984).

<sup>9</sup>A. Kana-ah, M. Deiri, B. C. Cavenett, N. D. Wilsey, and T. A. Kennedy, *J. Phys. C* **18**, L619 (1985).

<sup>10</sup>G. Feher, *Phys. Rev.* **114**, 1219 (1959).

<sup>11</sup>D. M. Hoffmann, B. K. Meyer, F. Lohse, and J.-M. Spaeth, *Phys. Rev. Lett.* **53**, 1187 (1984).

<sup>12</sup>K. M. Lee, *Rev. Sci. Instrum.* **53**, 702 (1982).

<sup>13</sup>T. E. Feuchtwang, *Phys. Rev.* **126**, 1628 (1962).

<sup>14</sup>Atomic hf constant for P, obtained from G. D. Watkins and J. W. Corbett, *Phys. Rev.* **134**, A1359 (1964).

<sup>15</sup>Atomic hf constant for In, obtained from A. K. Koh and D. J. Miller, *At. Data Nucl. Data Tables* **33**, 235 (1985).

<sup>16</sup>U. Kaufmann and J. Schneider, in *Advances in Solid State Physics*, edited by J. Treusch (Vieweg, Braunschweig, Germany, 1984), Vol. 20, p. 87.

<sup>17</sup>ENDOR results on the  $AsAs_4$  antisite have recently been interpreted by Hoffmann *et al.* [D. M. Hoffmann, J.-M. Spaeth, and B. K. Meyer, *Mater. Sci. Forum* **10-12**, 311 (1986)] to indicate that the antisite is perturbed by a nearby interstitial As atom along a  $\langle 111 \rangle$  axis. ENDOR of this fifth As neighbor has been detected and a resolved splitting of the four near-neighbor lines caused by the interstitial ion observed. We see no evidence of a fifth P neighbor in our spectrum and the inhomogeneously broadened P lines are symmetrical, with no evidence of structure. We note, however, that the splitting seen by these workers is only  $\sim 0.5$  MHz, so we cannot rule out such effects in our spectrum.

<sup>18</sup>A. Abragam and B. Bleaney, *Electron Paramagnetic Resonance of Transition Ions* (Clarendon, Oxford, 1970), Chap. 4.